Cr(VI) permanently binds to lipid bilayer throughout reduction process.

Michal Nowakowski [a], Anna Wiśniewska-Becker [b], Joanna Czapla-Masztafiak [a], Jakub Szlachetko [c], Andrzej Budziak[d], Żaneta Polańska [e], Zuzanna Pietralik-Molińska [e], Maciej Kozak [e] and Wojciech M. Kwiatek[a]

[a] *Institute of Nuclear Physics Polish Academy of Sciences, PL-31342 Krakow, Poland*

[b] *Jagiellonian University in Krakow, Faculty of Biochemistry, Biophysics and Biotechnology, PL-30387, Krakow, Poland*

[c] *Solaris National Synchrotron Radiation Centre, Jagiellonian University, 30-392 Krakow, Poland*

[d] *AGH University of Science and Technology, Faculty of Energy and Fuels, Krakow, Poland*

[e] *Adam Mickiewicz University in Poznan, Faculty of Physics, PL-61-614, Poznan, Poland*

**wojciech.kwiatek@ifj.edu.pl*

Supplementary Information

1. Liposome evaluation

1) Liposomal phase transition temperature determination

Measurements were carried out on the Fourier Transfer Infrared (FTIR) Bruker TENSOR 27 Spectrometer with the ATR Platinum attachment and temperature controller HAAKE DL 30. The spectrometer was equipped with a KBr beamsplitter and DLATGS detector. The measurements were performed in a spectral range of 3000-2800- cm^{-1} with a spectral resolution of 4 cm^{-1} and a temperature range from 2 °C to 40 °C. The data were analyzed using OPUS data processing software (Bruker Optics). The positions of characteristic bands

were obtained from the second derivative spectra. Liposomal phase transition temperatures were determined using Infrared spectroscopy based on the position of $\nu_s(CH_2)$ band.

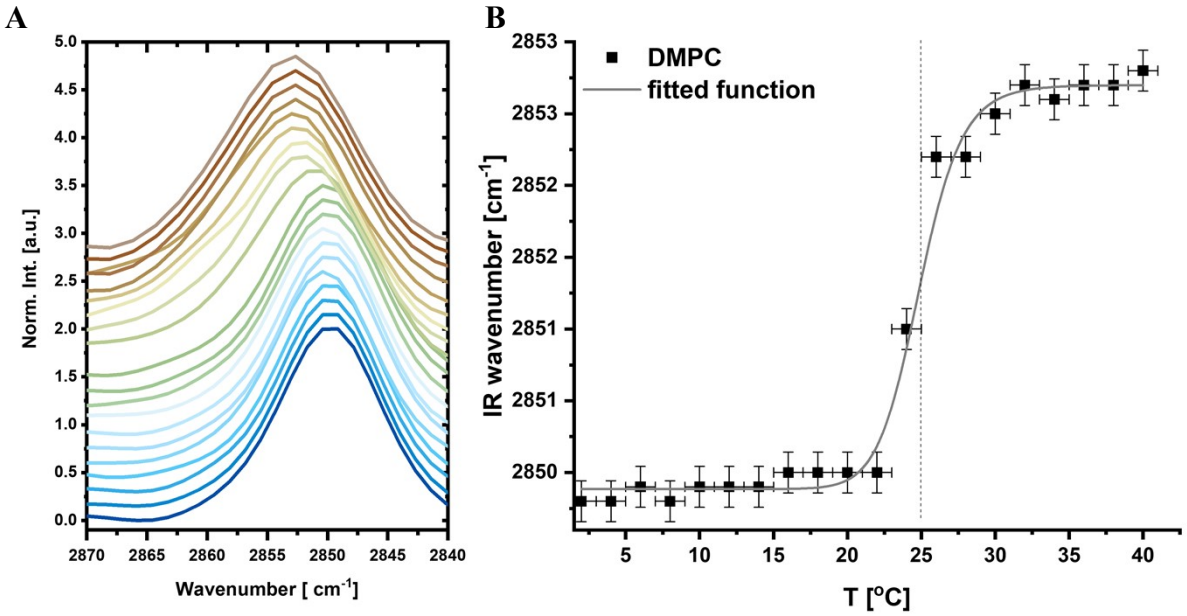

Fig. S1.1. Results of IR experiment for DMPC liposomes **A –** IR spectra stack-plotted as a function of temperature; **B -** the position of the $\nu_s(CH_2)$ band as a function of temperature. Vertical dashed line indicates an inflection point and a T_m.

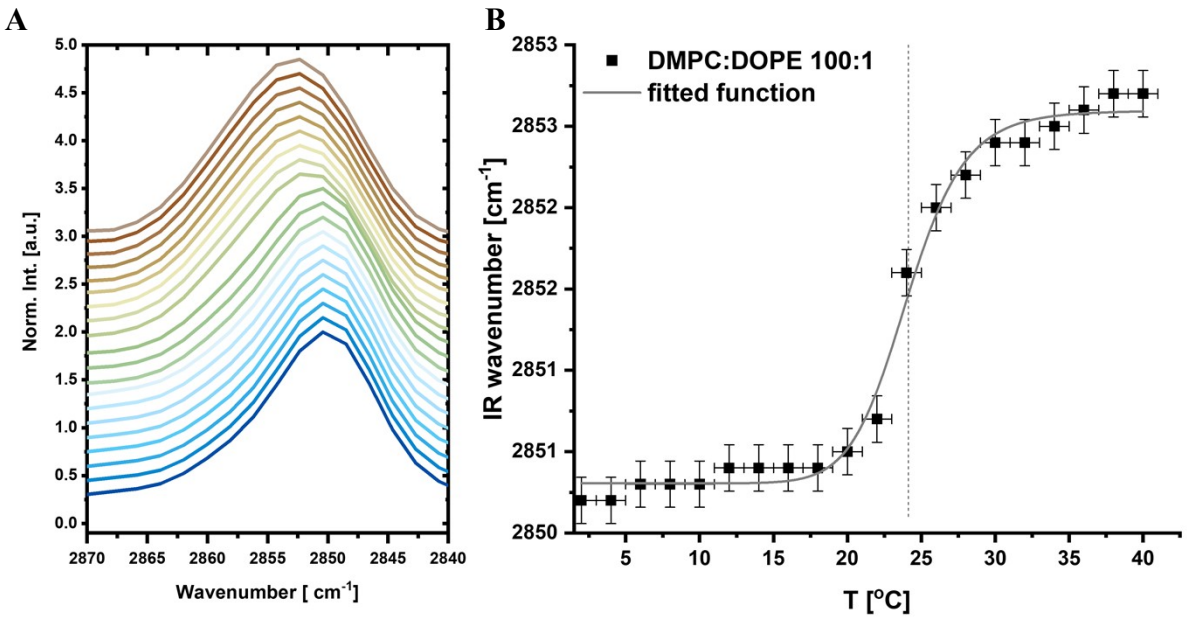

Fig. S1.2. Results of IR experiment for DMPC:DOPE 100:1 liposomes **A –** IR spectra stack-plotted as a function of temperature; **B -** the position of the $\nu_s(CH_2)$ band as a function of temperature. Vertical dashed line indicates an inflection point and a T_m.

28

29

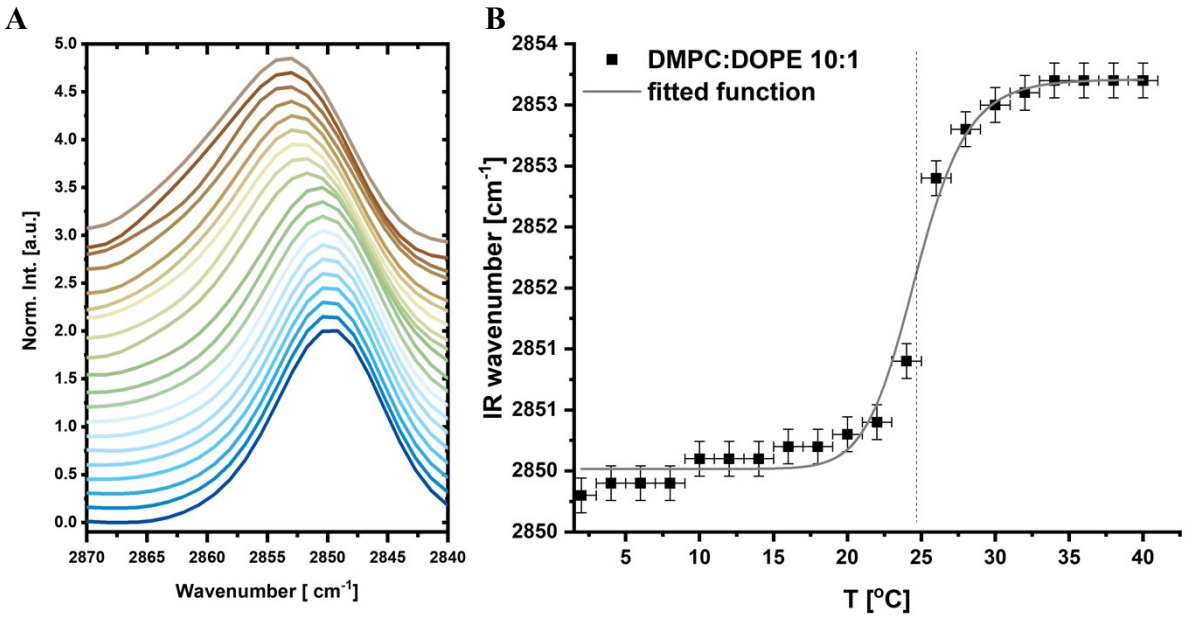

Fig. S1.3. Results of IR experiment for DMPC:DOPE 10:1 liposomes **A –** IR spectra stack-plotted as a function of temperature; **B -** the position of the $\nu_s(CH_2)$ band as a function of temperature. Vertical dashed line indicates an inflection point and a T_m.

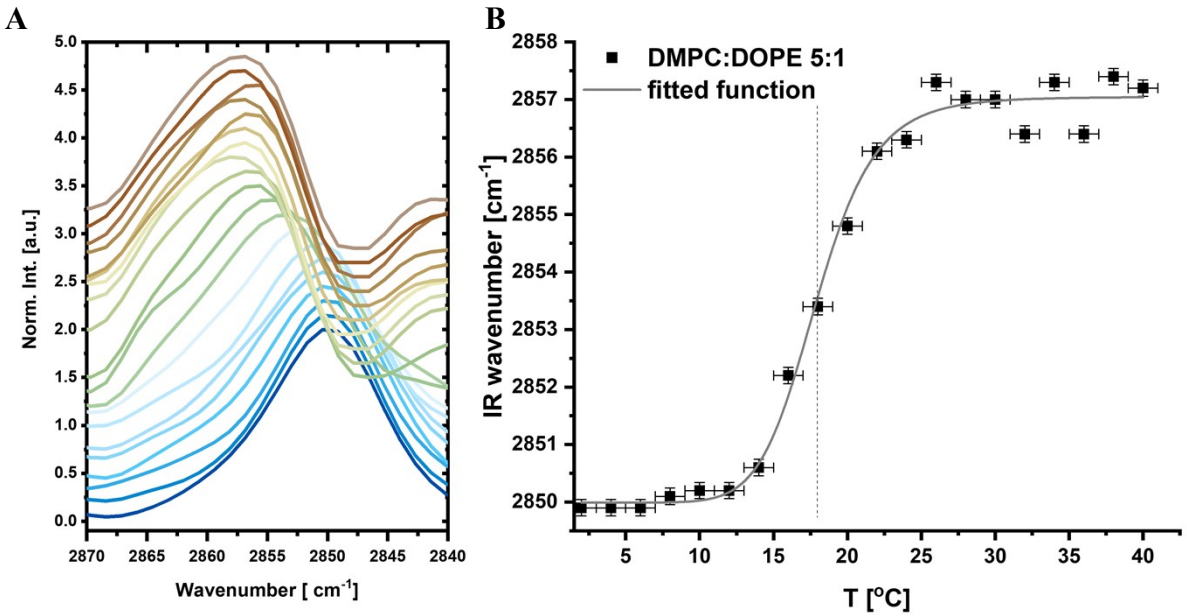

Fig. S1.4. Results of IR experiment for DMPC:DOPE 5:1 liposomes **A –** IR spectra stack-plotted as a function of temperature; **B -** the position of the $\nu_s(CH_2)$ band as a function of temperature. Vertical dashed line indicates an inflection point and a T_m.

30

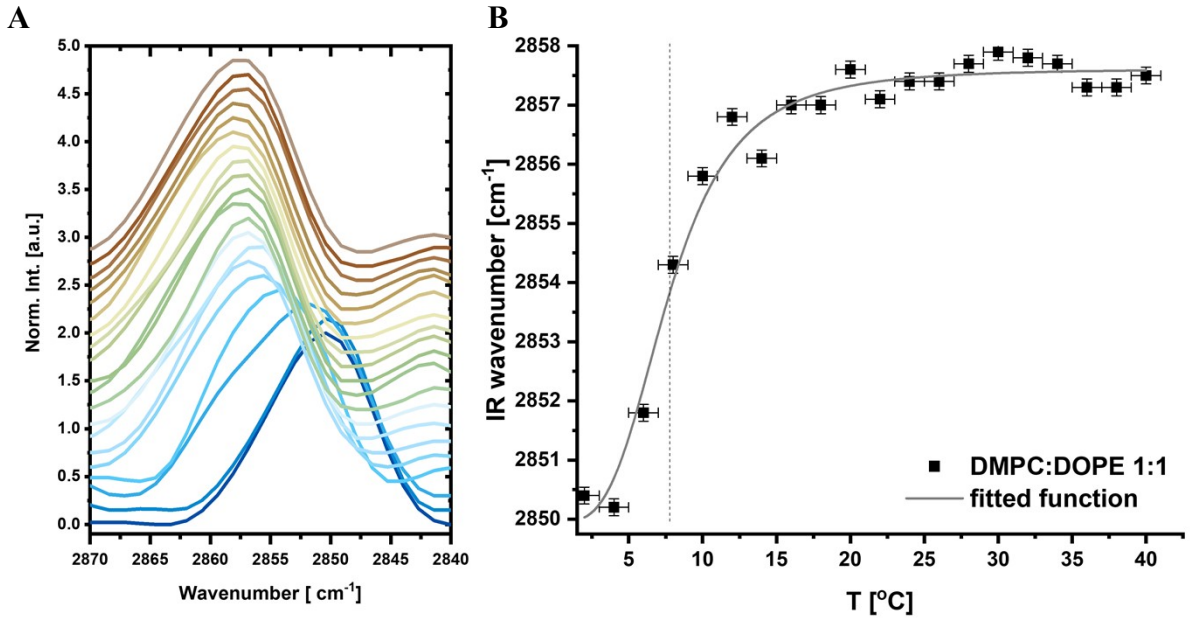

Fig. S1.5. Results of IR experiment for DMPC:DOPE 1:1 liposomes **A –** IR spectra stack-plotted as a function of temperature; **B -** the position of the $\nu_s(CH_2)$ bandas a function of temperature. Vertical dashed line indicates an inflection point and a T_m.

The collected FTIR spectra for DMPC are presented in Fig. S1.1A and spectra for liposomes with increasing DOPE content are presented in Fig. S1.2-1.5A. A fitting procedure determined the position of the $\nu_s(CH_2)$ band for each spectrum and the results were plotted as a band position as a function of temperature (Fig. S 1.1-1.5 B). As can be observed, $\nu_s(CH_2)$ bands are shifting toward higher wavenumbers as temperature increases. It is connected to the phase transition from the lamellar gel phase to the liquid crystal phase, where *trans-gauche* isomerization of aliphatic chains occurs[1]. A sigmoidal function shape was fitted to obtain the inflection point of the sigmoid curve, which indicated the T_c. One can see that the addition of DOPE is causing the decrease in the T_c value, which is the highest for pure DMPC liposomes. The presence of unsaturated acyl chains in DOPE molecules increases the membrane fluidity which causes the decrease of T_c. This behavior was already predicted for numerous liposomal mixtures [2].

Table S1.1 Phase transition temperatures determined by FTIR. The values in brackets indicate total uncertainty.

Liposomes	**Phase transition temperature T_c [°C]**
DMPC	24.9(4)
DMPC:DOPE 100:1	24.1(3)
DMPC:DOPE 10:1	24.7(4)
DMPC:DOPE 5:1	17.9(9)
DMPC:DOPE 1:1	7.7(1.3)

2) Phase transition enthalpy

Differential scanning calorimetry was used to determine the enthalpy of the relevant phase transitions as shown in Fig. S1.6. The transition enthalpies are shown in Table S1.2. Measurements were performed on a DSC-204 calorimeter, (Netzsch GmbH, Germany). Samples of 20 µl were closed in aluminum crucibles. Measurements were performed at the heating rate of 1 °C/min, in helium atmosphere (He flow rate: 40 mL/min). For each sample, two independent measurements were performed and the results were averaged. The data were analyzed using the TA Netzsch program. For the determination of enthalpy values characterizing phase transitions, a linear or a tangent-sigmoidal baseline was used.

Recorded DSC thermograms are presented in Fig S1.6 and determined parameters are summarized in Tab. S1.2. Thermogram for DMPC-based liposomes exhibits two phase transitions, the main transition and pretransition characterized by temperatures of 24.1 and 16.5 °C, respectively. These values are in good agreement with the literature [3]. The addition of DOPE causes the disappearance of the pretransition, a slight shift of the beginning of the main transition toward lower values, and a significant decline in the transition enthalpies values, which led to evanesce of the peak in the thermogram recorded for the system with the highest DOPE content. These changes indicate a decrease in the degree of cooperative of the transition

caused by the weakening of interactions between aliphatic chains due to the incorporation of the lipid molecules with unsaturated fatty acids between DMPC molecules [4][].

	T_m [°C]	T_{onset} [°C]	$\Delta T_{1/2}$ [°C]	ΔH [kJ/mol]
DMPC*	24.1	23.9	0.3	15.6
DMPC:DOPE 100:1	23.9	23.8	0.2	11.1
DMPC:DOPE 10:1	23.8	23.6	0.2	5.0
DMPC:DOPE 5:1	23.9	23.7	0.2	3.2
DMPC:DOPE 1:1	x	x	x	X

Table S1.2. Transition temperatures and enthalpies obtained for the studied liposomes.

*DMPC pretransition: T_p = 16.5°C, T_{onset} = 15.6°C, $\Delta T_{1/2}$ = 0.9°C, ΔH = 1.7 kJ/mol

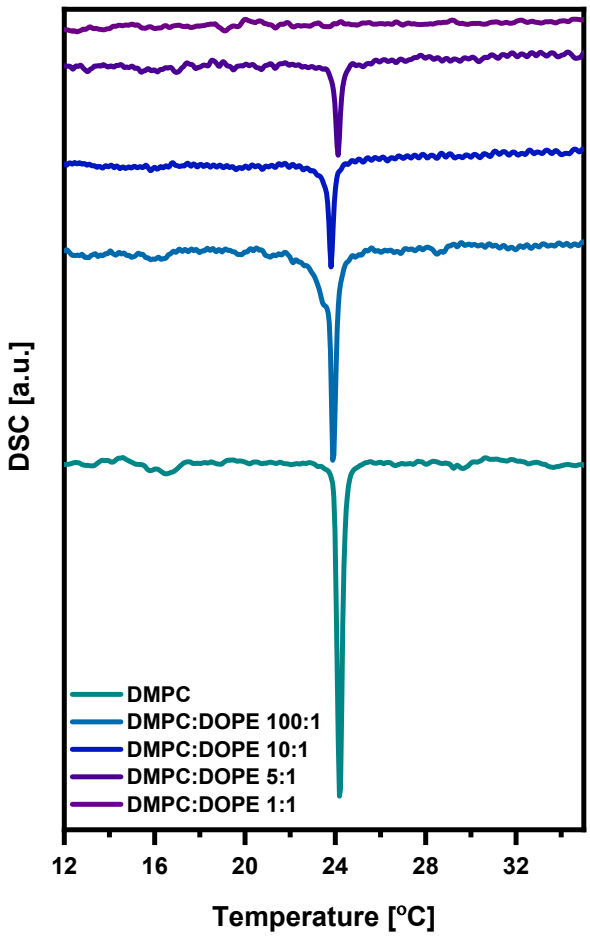

Fig. S1.6. Results of DSC measurements for liposomes based on DMPC with the increasing DOPE content.

3) Liposomal morphology study

For further evaluation of liposome morphology small angle X-Ray scattering measurements were performed at two temperatures: 15 °C and 30 °C, that is, below and above the detected phase transition temperature. Small angle X-ray scattering measurements were conducted using a XEUSS 2.0 system (XENOCS, France), equipped with MetalJet microfocus X-ray source ($\lambda = 0.134$ nm) with a liquid metal target (gallium/indium alloy) (Excillum AB, Sweden), PILATUS 3 R 1 M hybrid photon counting 2D detector (Dectris AG, Switzerland) and Fox 3D Ga ultra-low divergence mirrors (XENOCS, France). The sample-to-detector

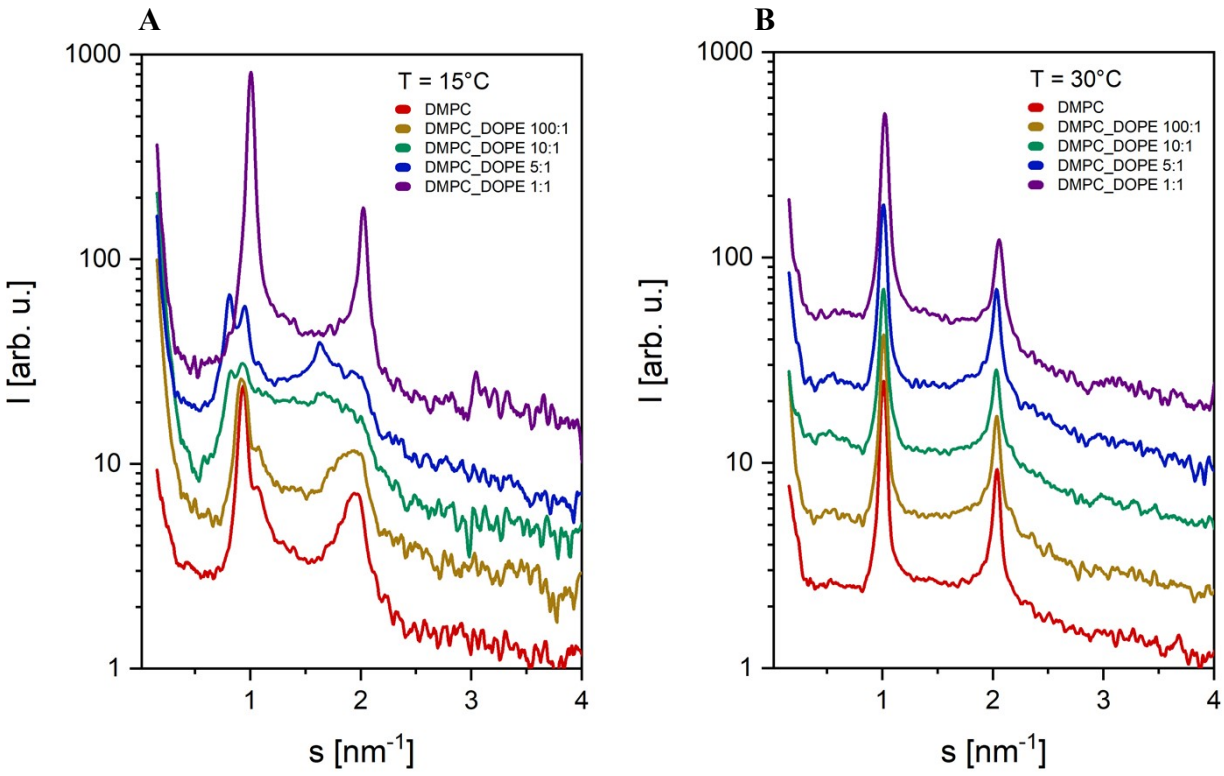

Fig. S1.7. Results of SAXS experiment for all studied liposomes **A** – Below T_c (15°C); **B** – Above T_c (30°C)

distance was 1686 mm and Linkam temperature attachment (Linkam Scientific Instruments Ltd., UK) and borosilicate glass capillaries (Hilgenberg GmbH, Germany) were used. For each sample, 12 frames (600 s/frame) were collected. Then all the collected frames were processed using FOXTROT processing softaware [5] and the buffer scattering was subtracted using PRIMUS [6] .

The results of SAXS experiments for systems with DMPC and DMPC:DOPE are shown in Fig S1.7. For temperature above T_c SAXS curves recorded for studied systems exhibit a lamellar structure characteristic for phospholipids with diffraction peaks appearing in relation to each other in a 1:2. For DMPC liposomes at a temperature above T_c, the intramolecular distances are d_{001} = 6.20 nm and d_{002} = 3.09 nm. These values remind unchanged upon the DOPE addition, only for the highest content of DOPE (1:1) a slight decrease is observed (d_{001} = 6.13 nm and d_{002} = 3.05 nm). Also, the intensity of the diffraction peaks is dependent on DOPE concentration which implies that the second lipid component has a destabilizing effect on the formed bilayer structures.

At temperature below T_c additional diffraction reflections are observed. This is clearly visible in SAXS curve record for the sample with 5:1 ratio of DMPC:DOPC. These peaks can be either attributed to two-phase separated lamellar structure with for different lipid composition and corresponding lattice parameters of 7.72 nm and 6.61 nm. However there is also possibility that the lamellar structure coexists with hexagonal phase characterised by intramolecular distances d_{100} = 6.6 nm, d_{110} = 3.79 nm, d_{200} = 3.29 nm (the ratio of 1:$\sqrt{3}$:2) and the calculated intercolumnar distance for this phase would be 7.64 nm. For the highest DOPE content, single lamellar structure is formed with d_{001} = 6.24 nm, d_{002} = 3.14 nm and d_{003} = 2.07

XRD experiment

Fig. S2 presents XRD patterns of Cr(VI)-untreated samples. One can see that there is a significant difference between DMPC and DMPC:DOPE liposomes even for the lowest DOPE content in terms of internal ordering. Table S1 presents detailed information regarding the most important and common for all spectra features of the XRD patterns discussed in the main text. Table S2 contains additional peaks identified in the XRD patterns in Fig S2. As indicated in the main text, in both groups, when Cr(VI) was added, an internal order of phospholipid bilayers has decreased except for the DMPC:DOPE 1:1 sample.

An average thickness of liposomal membranes with a large DOPE fraction (Fig. 1 b) decreased when samples were treated with a Cr(VI), while for liposomes with a small DOPE fraction, the effect was more subtle and opposite. For DMPC and DMPC:DOPE 100:1, very weak structures are present at a high angle limit of 2Θ. While for DMPC, there is one peak with a maximum of 2Θ at 28.18 ° (equal to 3.16 Å), for DMPC:DOPE 100:1, there are two maxima

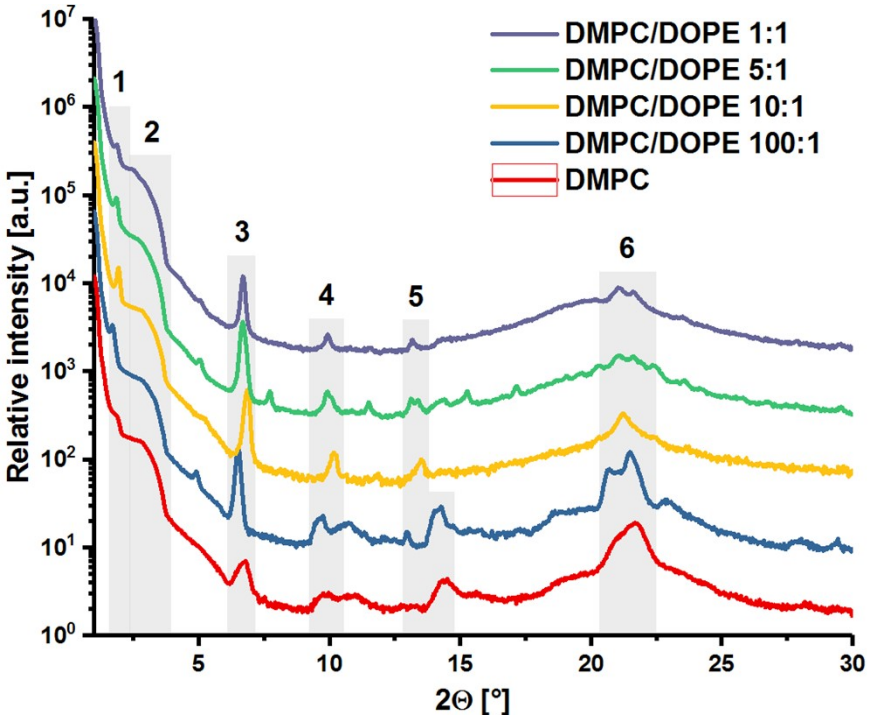

Fig. S2. X-Ray powder patterns of liposomal samples that were not treated by Cr(VI). Numbers are corresponding to peaks in Table 1, and grey areas indicate regions of interest.

116 at the 28.05 ° and 29.44 ° of 2Θ (equal to the 3.18 and 3.03 Å respectively). These features are

missing in the group with a high DOPE ratio (Fig. 1 b). For Cr(VI)-treated samples with a low DOPE fraction (Fig. 1 a), mentioned peaks are not visible. In turn, both samples exhibit two twin-like peaks that emerged with maxima at the 27.24 ° and 27.60 ° of *2Θ* (equal to the 3.27 and 3.23 Å respectively) for DMPC +Cr liposomes and 27.14 ° and the 27.48 ° of *2Θ* (equal to the 3.28 and 3.24 Å correspondingly) for the DMPC:DOPE 100:1 +Cr liposomes. The DMPC and DMPC:DOPE 100:1 liposomes had the least fluid membranes, and a Cr(VI) had little ability to penetrate lipid membranes compared to a high DOPE ratio group. The experiment was prepared so that Cr(VI) permeated throughout lipid membranes thanks to a force generated due to an imbalance of Cr(VI) concentration between the inside and outside of a liposome. We speculate that the permeation process started from an external surface of liposomes, yet the process was slowed down if the membrane was not fluid enough. Moreover, there was not enough target for oxidation (–HC=CH–) and the creation of a new ordered structure with a defined d_{hkl} value related to the oxidation product. Therefore, it is reasonable to associate the double peak in the DMPC +Cr and DMPC:DOPE 100:1 +Cr XRD patterns with a reaction

	6	5	4	3	2^b	2^a	1
	Peak position 2Θ [°]						
DMPC	21,69	14,44	9,86	6,68	3,71	2,81	1,88
DMPC/DOPE 100:1	21,49	14,27	9,76	6,52	3,71	2,88	1,71
DMPC/DOPE 10:1	21,23	13,51	10,16	6,85	3,71	2,84	1,94
DMPC/DOPE 5:1	21,13	13,37	9,93	6,69	3,71	2,88	1,81
DMPC/DOPE 1:1	21,06	13,14	9,93	6,69	3,75	2,91	1,88
	Peak position [Å]						
DMPC	4,09	6,13	8,96	13,22	23,77	31,39	47,06
DMPC/DOPE 100:1	4,13	6,20	9,05	13,54	23,77	30,67	51,66
DMPC/DOPE 10:1	4,18	6,55	8,69	12,88	23,77	31,03	45,44
DMPC/DOPE 5:1	4,20	6,61	8,90	13,20	23,77	30,67	48,70
DMPC/DOPE 1:1	4,21	6,73	8,90	13,20	23,56	30,31	47,06

a - beginning of a "bump"
b - end of a "bump"

Table S2 Main characteristic peak positions for all samples from Fig. S2. The table is divided to two groups with low and high DOPE fraction. Upper part of table shows results of 2Θ value in [°], while bottom part shows corresponding d_{hkl} values in [Å]. Positions of a characteristic "bump" shown in Fig. 1 is indicated by green background.

between Cr(VI) and the surface of membranes which, in turn, could increase the order on these surfaces.

The position of all main peaks marked in Fig S2 correlate with distinct parts of a bilayer: surface, –HC=CH– bond position, an interface between monolayers, and finally, the total bilayer thickness. For example, in the case of the DMPC:DOPE 1:1 sample main peaks in Table S1 are corresponding to the following distances: 4.2 Å, 6.7 Å, 8.9 Å, 13.2 Å, 23.6 Å, 30.3 Å, and 47.1 Å. Values of 8.9 Å and 13.2 Å correspond to a –C=C– bond position, while the value of 47.1 Å is comparable to a 2-fold value of a single monolayer thickness. Additionally, distances of 23.6 Å and 30.3 Å are comparable to a single monolayer thickness. It must be noted that there are similar relations between different reflections: 8.9/4.2 ≈ 2.1, 13.2/6.7 ≈ 2.0, 47.1/23.6 ≈ 2.0. These distances could be interpreted either as bilayer and monolayer characteristic d_{hkl} values or just the next-order X-Ray reflections (yet it does not change the general interpretation of the presented results). However, since peak shifts are not the same, we interpret these peaks as actual first-order XRD reflections. Finally, when Cr(VI) was added, the most pronounced changes were visible in a range of c.a. 47-40 Å, the "bump" and peak around the 6.6 Å, associated with a shape of whole bilayers.

The liposomes with the highest DOPE concentration exhibited different properties than other samples when treated with a Cr(VI). For the DMPC:DOPE 1:1 +Cr, an additional peak at 2.48 ° (35.58 Å) appeared (Fig. 1 B). Additionally, the most intense peak in the DMPC:DOPE 1:1 +Cr spectrum is split into two components with intensity maxima at 7.69 °, 6.69 ° (11.48 Å and 13.20 Å). A broad peak at 21.06 ° (4.21 Å) is singular for Cr(VI)-treated spectrum and was split for the DMPC:DOPE 1:1 pattern. While the broad feature cannot be precisely interpreted, splits around 7 and 2 ° could be associated with creating two co-existing phases of phospholipids, each of them created domains. Interestingly, all liposomes, regardless of DOPE

155 concentrations, had similar XRD patterns after a Cr(VI) treatment, except the region between
156 3.7 and 2.8 ° where the averaged structure is present.
157
158

2. XAS analysis

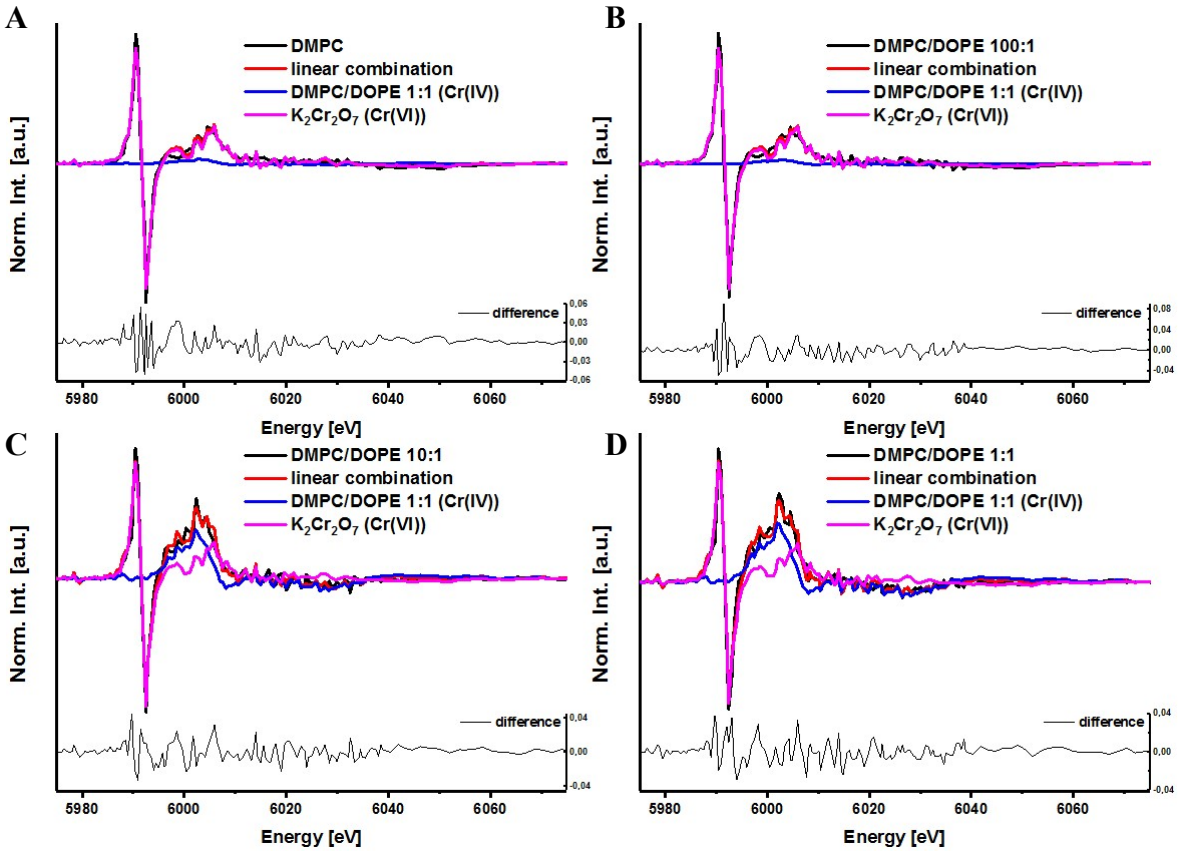

Fig. S3. Fitting results for liposomal samples. Since LCF was done on differentiated spectra, for purpose of presentation, energy ranges in this figures were cut only to important parts. LCF results for : A – DMPC liposomes; B – DMPC:DOPE 100:1 liposomes; C – DMPC:DOPE 5:1 liposomes; D – DMPC:DOPE 1:1 liposomes.

The experimental protocol for a pellet preparation contained a drying step at 55 °C. This step has extended an effective reaction process between the $K_2Cr_2O_7$ and liposomes from 15 minutes to approx. 12 h. Moreover, when water was removed, a local concentration of all reagents increased, thus shifting the reaction equilibrium: Cr(VI) + R ↔ Cr(III)–R into the product side. In general, it could lead to the production of new products. To rule out this possibility, we have performed quick XANES scans of liquid liposomal samples. Samples had the same composition as liposomes in pellets, yet the reaction time was precisely 15 minutes before the dialysis procedure stopped. We have compared outcome XANES spectra for pellets and suspension by

calculating differential spectra: $XAS^{lip} - XAS^{K2Cr2O7}$ (Fig. S3). No additional types of compounds were created during sample drying, which agrees with some literature reports about Cr(VI) interaction with lipid bilayers studied using EPR spectroscopy [7].

172 The comparison between samples measured in powder and solution is presented in Fig. S4.

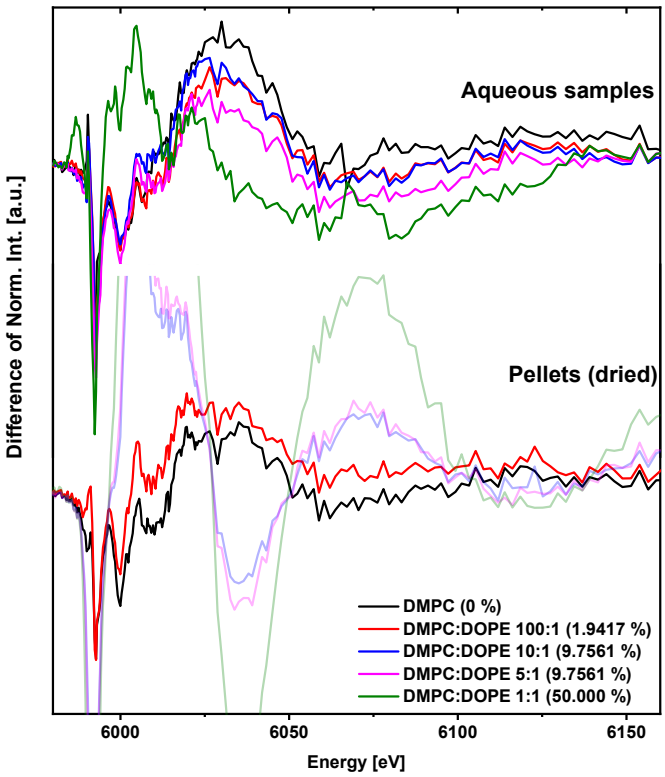

Fig. S4. Differential spectra calculated for both liposomal suspension and pellets as: sample – $K_2Cr_2O_7$. Spectra were normalized and smoothed in Athena software, using Gaussian filter with kernel size of 3 and width 10, prior to difference spectra calculation.

In the range of 5970-6055 eV for the aqueous DMPC, DMPC:DOPE 100:1, DMPC:DOPE 10:1, and DMPC:DOPE 5:1 changes are similar to these observed for the DMPC and DPMC/DOPE 100:1 for pellets. The main difference is due to the magnitude of changes observed. The aqueous DMPC:DOPE 1:1 sample has more Cr(VI) fraction of its counterpart from the pellet, which can also be seen in Table S3, and the presence of a feature around 6065 eV in Fig. S4. Values in Table S3 were obtained in the same LCF procedure as applied for the data in Table 1. Compared to results obtained from LFC presented in Table S3, there was much less reduction process in liquid samples. Due to the lower density of Cr in aqueous samples in general, there was a much worse S/N ratio, and subsequently, R values are worse, especially for the DMPC:DOPE 1:1 liposomes.

Sample	Cr reference		[Cr(VI)/Cr(IV)]	R
	$K_2Cr_2O_7$ (Cr(VI))	DMPC:DOPE 1:1 (Cr(IV))		
DMPC	0.899(19)	0.101(19)	8.901(1.863)	0.072
DMPC:DOPE 100:1	0.959(20)	0.041(20)	23.390(11.898)	0.075
DMPC:DOPE 10:1	0.969(21)	0.031(21)	31.258(21.852)	0.075
DMPC:DOPE 5:1	0.910(21)	0.090(21)	10.111(47)	0.094
DMPC:DOPE 1:1	0.786(25)	0.214(25)	3.673(546)	0.163

Table S3. LCF results for liquid samples. As previously, $K_2Cr_2O_7$ and DMPC:DOPE 1:1 samples were used as references for Cr(VI) and Cr(IV) respectively. The R value is fit evaluation and is defined as $R = \sum_i^N \frac{y_i - y_i'}{y_i^2}$ where N is a number of data points, y_i is a data point value and y_i' is fitted value at the same

XRF experiment details

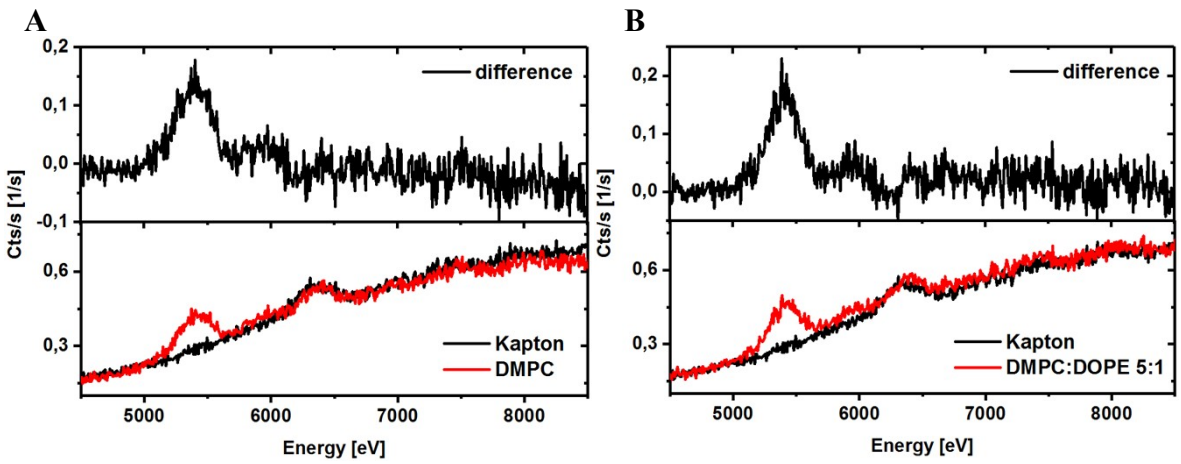

Fig. S5. Differential XRF spectra (top) for exemplary data from Fig. 4 obtained by subtracting the background spectrum liposomal one (bottom) for: A – DMPC +Cr liposomes; B – DMPC:DOPE 5:1 + Cr liposomes.

In the XRD experiment, the energy scale was spanned from 3.5 keV to 8.4 keV. The detection window was as such since for the energy lower than 1642 eV our setup would not resolve any characteristic fluorescence, and no interesting signal was expected. Additionally, a background contribution was very high in the 0 – 1500 eV region. We have used a 30 kV voltage with ~20 μA lamp current. An additional collimating Pb tube suppressed strong Fe, Cu, and Ni peaks originating from the experimental setup (background, Fig. 4). From all liposomal and reference spectra, the background spectrum (a Kapton foil) was subtracted, and all residual peaks originated from the local environment were removed as well as a baseline was improved (examples: Fig. S5 a-b). A Gaussian peak function was fitted to Cr Kα emission lines using OriginPro 9.1 Sr2 (*OriginLab Corporation*) software. All XRF spectra were normalized by values of the detector *Real time* to obtain values in *[cts/s]*. Finally, the calibration curve was fitted using a linear regression method for values obtained from $K_2Cr_2O_7$, $CrCl_3$ x $5H_2O$, Cr_2O_3 references. As mentioned before, to fit liposomal samples into a cryostat holder, we had to cut them. Thus, in the XRF experiment, we had only parts of the samples measured in the XAS experiment. To overcome this problem, we have calculated a correction factor for all samples,

based on the studied sample area. To do this, we took high-resolution photographs of all DMPC:DOPE + Cr pellets in high contrast and under the same conditions. Next, using GNU Image Manipulation Program (GIMP) 2.8.16 (*Spencer Kimball, Peter Mattis and the GIMP Development Team*) color selection tool ("Fuzzy Selection Tool") set to 7 px threshold, we have selected all parts of the image with black color. A binary image was created and further opened in ImageJ 1.49v (*Wayne Rasband, National Institute of Health, USA*) software [8]. The pellet area was counted using the option Analyze -> Analyze Particles. Results for liposomal samples were compared with an undamaged reference Cr_2O_3 pellet, and the correction factor for each sample was calculated. Obtained correction allowed us to calculate the total Cr content inside liposomal samples.

References

1 R. N. A. H. Lewis and R. N. Mcelhaney, *BBA - Biomembranes*, 2013, **1828**, 2347–2358.

2 R. Koynova and M. Caffrey, .

3 M. Caffrey and J. Hogan, *Chem Phys Lipids*, 1992, **61**, 1–109.

4 C. Demetzos, *J Liposome Res*, 2008, **18**, 159–173.

5 R. Girardot, G. Viguier, J. Pérez and M. Ounsy, in *Proceedings of the 8th canSAS Meeting*, Tokai, Japan, 2015.

6 P. V. Konarev, V. V. Volkov, A. V. Sokolova, M. H. J. Koch and D. I. Svergun, *urn:issn:0021-8898*, 2003, **36**, 1277–1282.

7 J. Belagyi, M. Pas, P. Raspor, M. Pesti and T. P??li, *Biochim Biophys Acta Biomembr*, 1999, **1421**, 175–182.

8 C. A. Schneider, W. S. Rasband and K. W. Eliceiri, *Nature Methods*, 2012, **9**, 671–675.